A closed form solution for the vulcanization prediction of NR cured with sulphur and different accelerators

G. Milani · T. Hanel · R. Donetti · F. Milani

Received: 31 July 2014 / Accepted: 9 December 2014 / Published online: 17 December 2014

1 Introduction

The vulcanization with sulphur of natural rubber (NR) is particularly complex. This is the reason why, despite its first practical application dates back to the second half of nineteenth century, its chemical mechanisms are not still completely understood. Due to such theoretical lack, it remains difficult to develop efficient numerical tools to optimize the vulcanization process of items with big dimensions and to predict their final elasto-mechanical properties.

As well known, the crosslink density may be indirectly estimated by means of many macroscopic procedures, but the most diffused and simple one is the so-called rheome-ter test. A rheometer is a laboratory device where a small rubber sample is subjected to constant cure temperature and the torque applied to maintain a constant rotation of the moving part (e.g. oscillating disc, moving die, etc.) is measured. The torque generally starts to increase very slowly (or decreases) during an "induction" period of time, after which the main vulcanization reaction takes place with a significantly faster increase of the crosslink density and hence of the measured torque within the rheometer. Very frequently, for NR vulcanized with sulphur, it can occur that torque reaches a max-imum and then starts to decrease, resulting in weaker mechanical properties of the vulcanizate for long curing times. This last phenomenon, called "reversion", is well known for sulfur cured rubbers at high vulcanization temperatures (typically above 140 °C) and is attributed to the formation and subsequent degradation of polysuldic (S–S or more) crosslinks [1–3]. Generally, in sulphur vulcanized rubber, it is com-monly accepted that there are three types of polysulfidic structures namely C–S–C, C–S_2–C and C–S_x–C.

The primary reaction leading to polysulfidic structures involves the formation of reactive crosslinking precursors (which can contain between 2 and 8 S–S links) on a rubber chain by reaction with sulphurating agents. This precursor can then react either with another rubber chain, resulting in a crosslink, or with the same rubber chain, by a backbiting reaction resulting in a cyclic structure. In this latter case, the polysulfidic structure does not contribute to the increase of the crosslink density.

The evidence for these polysulfidic structures (both crosslinking and cyclic ones) is provided by an important physical chemistry literature, obtained by IR, UV, ESR and Raman characterizations [4,5] or with chemical methods [6], or by means of solid

G. Milani (✉)
Politecnico di Milano, Piazza Leonardo da Vinci 32, 20133 Milan, Italy
e-mail: milani@stru.polimi.it; gabriele.milani@polimi.it

T. Hanel · R. Donetti
Pirelli Tyre, Via Alberto e Piero Pirelli 25, 20126 Milan, Italy

F. Milani
Chem.Co Consultant, Via J.F.Kennedy 2, 45030 Occhiobello, RO, Italy

state ^{13}C nuclear magnetic resonance (NMR) studies [7], as done for instance in [8,9] for EPDM. In this latter case, the polysulfidic structures are consistent with predictions based on model compounds and the presence of three different allylic positions in the repeating unit of NR [7]. The percentages of each polysulfidic structure and the value of x depends on both rubber structure and reaction conditions, the most important being temperature and curing time [10]. It has been observed experimentally, that in the initial stage of the reaction, more crosslinking C–S_x–C ($x = 4$, 5 or more) bonds are found. It is generally assumed that (C–S_x–C) polysulfidic crosslinks can further react, leading either to shorter crosslinks (C–S–C), through a so called "maturation reaction", or to cyclic polysulfidic structures by backbiting reactions. In such a case, the crosslink density decreases, and this chemically explains the macroscopically observed reversion.

In practice, it has been observed that the importance of the reversion depends strictly on curing temperature. Nevertheless, recent results by Leroy et al. [11] and Milani et al. [12,13] tend to demonstrate that the ratio between thermally stable (short) and unstable (long) polysulfidic crosslinks is not significantly influenced by cure temperature.

The existing models that allow predicting such specific behavior regarding the kinetics of rubber vulcanization, by means of either a mechanistic (model of Coran [3], Ding and Leonov [14,15]) or a semi-mechanistic (model of Han et al. [16]) base, suffer from important limitations, such as the need of evaluating kinetic constants by best fitting numerical procedures on the available experimental data and the generalist point of view, which does not take into account the actual accelerators present in the system.

Recently, Leroy et al. [11] derived a phenomenological model with the same formalism of Han et al. [16] and Colin et al. [17], which gives a continuous prediction of the induction/vulcanization/reversion sequence. Similar approaches following the same scheme may be also found in [12,13]. Essentially, the phenomenological model proposed in [11] assumes that the during the induction and vulcanization steps, the overall formation of sulphur crosslinks can be described by a classic Kamal and Sourour formulation [18], which supposes a catalytic and autocatalytic second order apparent reaction mechanism. Consequently, despite its practical interest for numerical simulations, such a phenomenological model remains not fully predictive, since it does not allow relating the global reaction kinetics to the current knowledge of the different individual reactions involved. The procedure has been recently refined by Milani et al. in [19], where a complex kinetic scheme with seven constants is proposed, describing reversion by means of the distinct decomposition of single/double and multiple S–S bonds. The limitation of [19] model remains however the need of solving numerically a differential equations system, evaluating the kinetic constants by means of a least squares procedure.

In the present paper, a novel and efficient closed form approach to determine the degree of vulcanization of NR cured with sulphur in presence of more than one accelerator is presented. The general reaction scheme proposed by Han and co-workers for vulcanized sulphur NR is assumed as the initial base to develop a suitably modified new model accounting for the single contributions of the different accelerators, focusing in particular on some experimental data [20], where a NR has been vulcanized at different temperatures (from 150 to 180 °C) and concentrations of sulphur, using

TBBS (*N* terbutyl, 2 benzothiazylsulphenamide) and DPG (*N*,*N* diphenyl guanidine) as co-agents at variable concentrations.

In the model, chain reactions initiated by the formation of macro-compounds responsible for the formation of the unmatured crosslinked polymer are accounted for. It is assumed that such reactions depend on the reciprocal concentrations of all components and their chemical nature. In presence of two accelerators, reactions are assumed to proceed in parallel, making the assumption that there are no cross-reactions between the two accelerators. Despite there is experimental evidence of the existence of a process by which each accelerator affects the other, the reaction chemistry is still not well understood. For this reason, its real effect on vulcanization cannot be translated into any mathematical model. In any case, even disregarding such interaction, authors experienced a good numerical performance of the model on fitting experimental rheometer curves. From the kinetic scheme adopted, a closed form solution is found for the crosslink density, with the only limitation that the induction period is excluded from computations.

The main novelty of the model stands however in the closed form determination of the kinetic constants representing the rates of the single reactions in the kinetic scheme adopted. Such very straightforward procedure allows avoiding the utilization of numerically demanding least-squares best fitting routines on rheometer experimental data.

Two series of experiments available, relying into rheometer curves at different temperatures and different concentrations of sulphur and accelerators, are utilized to evaluate the fitting capabilities of the mathematical model. Very good agreement between numerical output and experimental data is experienced in all cases analyzed. The evaluation of kinetic constants at three vulcanization temperatures, after proper check of the linearity in the Arrhenius space, allows performing numerical simulations at curing temperatures outside the range experimentally inspected, making the model predictive in all those cases where a wide experimental campaign is not possible.

2 Experimental results

As base for the comprehensive validation of a newly conceived kinetic scheme ad-hoc developed by the authors, some experimental results [20] consisting of standard rheometer curves (MD rheometer tests) for NR vulcanized in various conditions have been considered.

The analyses focus on NR with different concentrations of S, TBBS and DPG at different temperatures. In particular, the same NR blend, with composition as in Table 1, was vulcanized with 9 different S–TBBS–DPG mutual concentrations, at four increasing curing temperatures equal to 150, 160, 170 and 180 °C. The final aim was to conduct a wide sensitivity analysis to have an experimental insight into the role played by the mutual concentration of the different accelerations on the (1) vulcanization level at the end of curing, (2) reaction velocity after scorch and (3) amount of reversion at different temperatures. The experimental campaign was designed in the S–TBBS–DPG space moving on the corners of the parallelepiped depicted in Fig. 1, with values of concentration (in phr) kept from previous experience of the authors in this field. A

Table 1 NR blend composition (in phr) considered in the numerical simulations simulations (zinc octoate at 3 phr was used in all cases)

Ingredients	(3,3,4) blend	(1,1,1) blend
NR	100	100
S	3	1
TBBS	3	1
DPG	4	1

NR Natural rubber SMR GP, *S* soluble sulphur, *TBBS N* terbutyl 2 benzothiazylsulphenamide, *DPG N,N* diphenyl guanidine

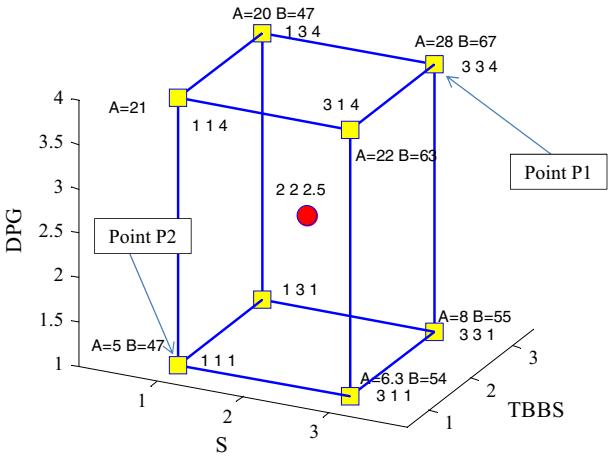

Fig. 1 Sensitivity experimental analysis conducted on a same NR blend. Corners and centroid of the parallelepiped represent S–TBBS–DPG concentrations experimentally tested at four different temperatures. Letters A and B represent the experimental % reversion at 8 min at 150 and 180 °C, respectively

further set of rheometer curves at different temperatures was obtained considering the centroid of the parallelepiped, with the aim of evaluating the curing behaviour at an intermediate situation.

Since the discussion of the experimental results and the systematic application of the numerical model based on experimental data is the object of a parallel study [20], here the model is validated only on two corners of the parallelepiped for the sake of conciseness. In particular, points P1 and P2 in Fig. 1 are considered, corresponding to S–TBBS–DPG concentrations equal to 3-3-4 and 1-1-1, respectively. For the sake of clearness from here ongoing, point P2 system will be named with NR+(S,TBBS,DPG)(1,1,1) and point P1 with NR+(S,TBBS,DPG)(3,3,4).

In Tables 2 and 3 a synopsis of the main properties exhibited by the rheometer curves is provided, as for instance time at which the maximum torque is reached, the value of the maximum torque, accelerators concentrations and curing temperature.

Crude experimental data obtained in the rheometer chamber are provided in Fig. 2 for (NR+(S,TBBS,DPG)(3,3,4) system and Fig. 3 for NR+(S,TBBS,DPG)(1,1,1).

Table 2 Rheometer curves NR+(S,TBBS,DPG)(3,3,4) system

T curing	150	160	170	180
S phr	3	3	3	3
[S]	9.40×10^{-2}	9.40×10^{-2}	9.40×10^{-2}	9.40×10^{-2}
TBBS phr	3	3	3	3
[TBBS]	1.02×10^{-2}	1.02×10^{-2}	1.02×10^{-2}	1.02×10^{-2}
DPG phr	4	4	4	4
[DPG]	1.89×10^{-2}	1.89×10^{-2}	1.89×10^{-2}	1.89×10^{-2}
(TBBS + DPG)/S	2.33	2.33	2.33	2.33
([TBBS] + [DPG])/[S])	2.47	2.47	2.47	2.47
% reversion 8 min	20	40	56	67
t max [min]	3.2	2	1	0.8
Torque max	6.4	6.4	6.4	6.4

Table 3 Rheometer curves NR+(S,TBBS,DPG)(1,1,1) system

T curing	150 °C	160 °C	170 °C	180 °C
S phr	1	1	1	1
[S]	3.12×10^{-2}	3.12×10^{-2}	3.12×10^{-2}	3.12×10^{-2}
TBBS phr	1	1	1	1
[TBBS]	0.34×10^{-2}	0.34×10^{-2}	0.34×10^{-2}	0.34×10^{-2}
DPG phr	1	1	1	1
[DPG]	0.47×10^{-2}	0.47×10^{-2}	0.47×10^{-2}	0.47×10^{-2}
(TBBS + DPG)/S	2	2	2	2
([TBBS] + [DPG])/[S])	2.1	2.1	2.1	2.1
% reversion 8 min	0	12	30	48
t max [min]	7.75	4.5	2.92	1.61
Torque max	4.2	4.1	3.9	3.77

A normalization of crude experimental curves is necessary to apply the numerical model proposed hereafter, with the preliminary exclusion of the induction period.

One of the most diffused methods to heuristically link the vulcanization degree with experimental rheometer torque is the Sun and Isayev [21] procedure. In [21], the $S'(t)$ torque is used as a measure to calculate the evolution of the vulcanization degree $\alpha_{exp}(t)$ through the following formula:

$$\alpha_{exp}(t) = \frac{S'(t) - S_{min\,T}}{S_{max\,T_0} - S_{min\,T_0}} \tag{1}$$

where:

– $S_{min\,T}$ is the minimum value of torque S' during a cure experiment at temperature T. Before reaching this minimum value, α_{exp} is considered equal to zero.

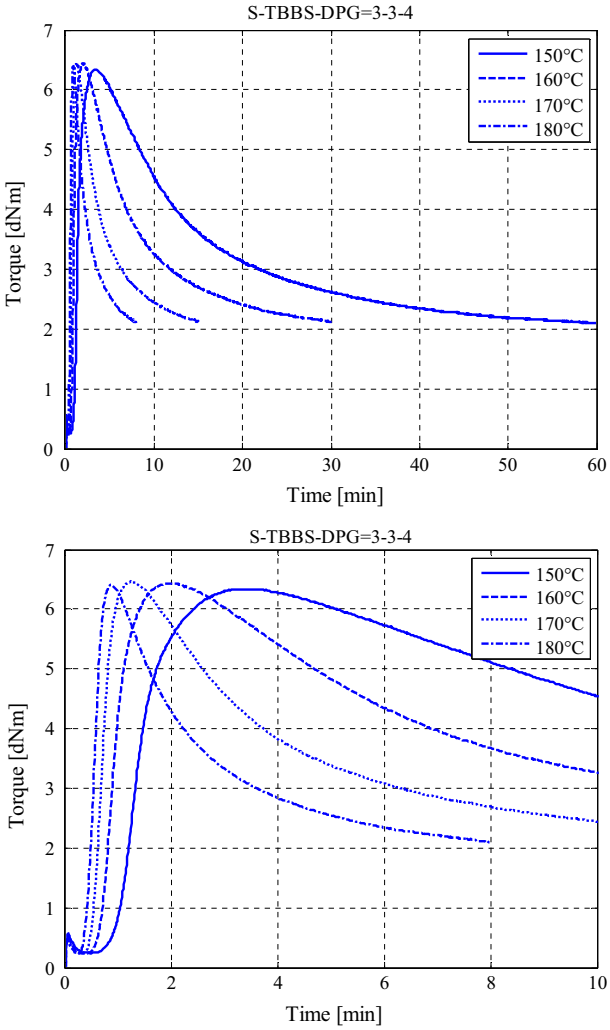

Fig. 2 Experimental rheometer curves, Table 2 dataset 1

– $S_{min\,T0}$ and $S_{max\,T0}$ are the minimum and maximum torque values, obtained for a cure experiment at a temperature T_0 low enough to allow neglecting reversion. In other words, the low temperature "reversion free" increase of mechanical properties during cure is taken as a reference, to estimate the influence of reversion at higher temperatures, which results in a final degree of vulcanization lower than 100 %.

In the present paper, a more straightforward but still effective normalization approach is adopted, relying into the exclusion from computations of rheometer data before scorch time and into the normalization of the torque values with the maximum

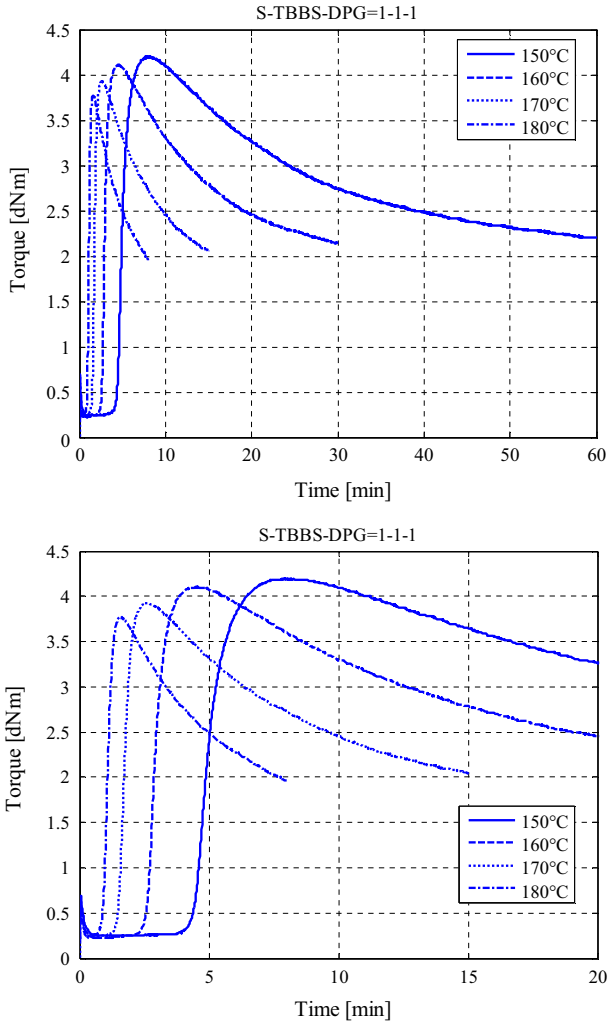

Fig. 3 Experimental rheometer curves, Table 3 dataset 2

torque reached at that temperature. In other words, the following formula for α_{exp}(t) is utilized:

$$\alpha_{\text{exp}}(t) = \frac{S'(t) - S_{\min T}}{S_{\max T} - S_{\min T}} \tag{2}$$

Note that using Eq. (2), $\alpha_{\text{exp}}(t)$ is always between 0 and 1 at each temperature, whereas using Eq. (1) it may occur that the maximum value of $\alpha_{\text{exp}}(t)$ is sensibly lower than 1, especially for high vulcanization temperatures.

A comparison of the two normalization procedures for the two cases analyzed in the paper is provided in Fig. 4. The induction period before the scorch time is still present, but no difference occurs if such data are deleted from the computations before

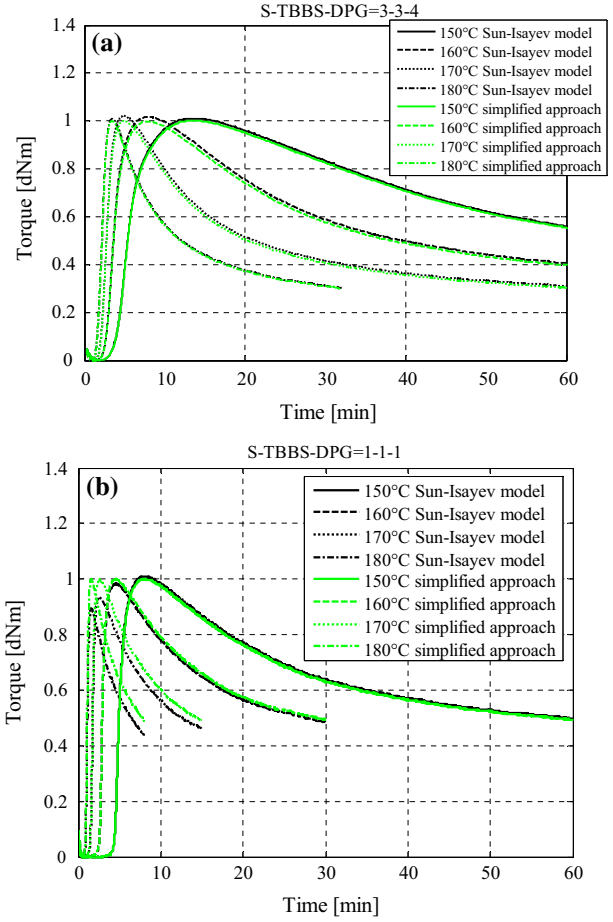

Fig. 4 Comparison of experimental rheometer curves normalization by means of Eqs. (1) and (2). **a** NR+(S,TBBS,DPG)(3,3,4) system. **b** NR+(S,TBBS,DPG)(1,1,1) system

or after normalization. As can be noted, the difference is practically negligible (lower than 10 % in the most unfavorable case, NR+(S,TBBS,DPG)(1,1,1) system at 150 °C) for all the curves considered. For this reason, the second normalization procedure is adopted for the sake of simplicity.

3 Revised kinetic scheme and mathematical closed form model

The basic reaction schemes assumed are classic and refer to existing literature in the field. Such schemes are known from the scientific literature, as mentioned above, see for instance [11,14,16,19,22].

As universally accepted, many reactions occur in series and parallel during NR cured with sulphur. Typically, the chain reactions are initiated by the formation of

macro-radicals or macro-ions representing the intermediate cross-link precursor. Such reaction is associated to a velocity represented by the kinetic constant k_1.

The actual cross-linking proceeds through two pathways, which have been shown to be additive, namely the formation of the unmatured crosslinked polymer and backbiting. In the first case, multiple S–S bonds on two contiguous polymer chains, whereas backbiting occurs when S–S bonds in the same back-bond chain. Since a multiple S–S bond is unstable, unmatured crosslinked polymer evolves either to matured crosslinked polymer exhibiting a single S or double bond between chains or leading to break of the bond and hence de-vulcanization, which occurs again with a backbiting of the bond in the same backbone chain. Potential interactions between DPG and TBBS can be hardily translated into mathematics and for this reason they are excluded from the model. All the reactions considered occur with a kinetic velocity depending on the temperature reaction, associated to each kinetic constant.

Let us assume that k_i and k_i' are the i-th kinetic constant associated to TBBS and DPG respectively and that index 1 (2) refers to concentrations of a chemical quantity reacting/formed with TBBS (DPG).

Within such assumptions, we adopt for NR the kinetic scheme constituted by the chemical reactions summarized in the following set of equations:

$$\begin{aligned}
&[TBBS] + [S_1] \xrightarrow{k_0} \left[A_1^*\right] \\
&[DPG] + [S_2] \xrightarrow{k_0'} \left[A_2^*\right] \\
&\left[A_1^*\right] \xrightarrow{k_1} \left[R_1^*\right] \\
&\left[A_2^*\right] \xrightarrow{k_1'} \left[R_2^*\right] \\
&\left[A_1^*\right] \xrightarrow{k_2} [R_1] \\
&\left[A_2^*\right] \xrightarrow{k_2'} [R_2] \\
&[R_1] \xrightarrow{k_3} \left[R_1^D\right] \\
&[R_2] \xrightarrow{k_3'} \left[R_2^D\right]
\end{aligned} \tag{3}$$

In Eq. (3), $[S_1]$ and $[S_2]$ are sulphur concentrations reacting with TBBS and DPG respectively, $\left[A_1^*\right]$ and $\left[A_2^*\right]$ the sulphurating agents, $\left[R_1^*\right]$ and $\left[R_2^*\right]$ the stable crosslinked chain (S–S single bonds), $[R_1]$ and $[R_2]$ the unstable vulcanized polymer, $\left[R_1^D\right]$ and $\left[R_2^D\right]$ the de-vulcanized polymer fraction (reversion). $k_{0,1,2,3}$ and $k'_{0,1,2,3}$ are kinetic reaction constants. Here it is worth emphasizing that $k_{0,1,2,3}$ and $k'_{0,1,2,3}$ are temperature dependent quantities, hence they rigorously should be indicated as $k_{0,1,2,3}\,(T)$ and $k'_{0,1,2,3}\,(T)$, where T is the absolute temperature. In what follows, for the sake of simplicity, the temperature dependence will be left out.

Once established the stoichiometric ratio between sulphur reacting with TBBS and DPG respectively, $\left[A_1^*\right]$ and $\left[A_2^*\right]$ sulphurating agents follow two parallel and independent pathways.

k_0 and k_0' are kinetic constants representing the induction period, that can be excluded from the computations assuming that the induction is evaluated by means of a first order Arrhenius equation.

According to the reaction scheme (3), the following differential equations may be written:

$$\begin{aligned}
&\text{(a)}\ \frac{d\left[A_1^*\right]}{dt} = -\left(k_1 + k_2\right)\left[A_1^*\right] \\
&\text{(b)}\ \frac{d\left[R_1^*\right]}{dt} = k_1\left[A_1^*\right] \\
&\text{(c)}\ \frac{d\left[R_1\right]}{dt} = k_2\left[A_1^*\right] - k_3\left[R_1\right]
\end{aligned} \tag{4}$$

Equation (4)(a) may be trivially solved by separation of variables, as follows [23]:

$$\begin{aligned}
&\text{(a)}\ \left[A_1^*\right] = \left[A_1^*\right]_0 e^{-(k_1+k_2)(t-t_i)} \\
&\text{(b)}\ \frac{d\left[R_1^*\right]}{dt} = k_1\left[A_1^*\right]_0 e^{-(k_1+k_2)(t-t_i)} \\
&\text{(c)}\ \frac{d\left[R_1\right]}{dt} = k_2\left[A_1^*\right]_0 e^{-(k_1+k_2)(t-t_i)} - k_3\left[R_1\right]
\end{aligned} \tag{5}$$

and, once known analytically $\left[A_1^*\right]$ function, it can be substituted into equations (b) and (c) to provide $\left[R_1^*\right]$ and $[R_1]$:

$$\begin{aligned}
&\text{(a)}\ \left[R_1^*\right] = \frac{k_1\left[A_1^*\right]_0}{k_1 + k_2}\left[1 - e^{-(k_1+k_2)(t-t_i)}\right] \\
&\text{(b)}\ \frac{d\left[R_1\right]}{dt} + k_3\left[R_1\right] = k_2\left[A_1^*\right]_0 e^{-(k_1+k_2)(t-t_i)}
\end{aligned} \tag{6}$$

(6)(b) is a non homogeneous first order linear differential equation, which admits the following solution composed by a general and a particular root:

$$\left[R_1\right] = \frac{k_2}{k_1 + k_2 - k_3}\left[A_1^*\right]_0\left[e^{-k_3(t-t_i)} - e^{-(k_1+k_2)(t-t_i)}\right] \tag{7}$$

The final concentration vulcanized polymer (related to TBBS) is thus $\left[R_1^*\right] + [R_1]$:

$$\begin{aligned}
\left[R_1\right] + \left[R_1^*\right] = &\frac{k_1\left[A_1^*\right]_0}{k_1 + k_2}\left[1 - e^{-(k_1+k_2)(t-t_i)}\right] \\
&+ \frac{k_2}{k_1 + k_2 - k_3}\left[A_1^*\right]_0\left[e^{-k_3(t-t_i)} - e^{-(k_1+k_2)(t-t_i)}\right]
\end{aligned} \tag{8}$$

Which can be normalized with respect to $\left[A_1^*\right]_0 = \beta\,[S]_0$ as follows:

$$r_1 = \frac{[R_1] + \left[R_1^*\right]}{[S]_0} = \beta \left\{ \frac{k_1}{k_1 + k_2} \left[1 - e^{-(k_1+k_2)(t-t_i)}\right] + \frac{k_2}{k_1 + k_2 - k_3} \left[e^{-k_3(t-t_i)} - e^{-(k_1+k_2)(t-t_i)}\right] \right\} \tag{9}$$

Analogously, for DPG we can find that:

$$r_2 = \frac{[R_2] + \left[R_2^*\right]}{[S]_0} = (1-\beta) \left\{ \frac{k_1'}{k_1' + k_2'} \left[1 - e^{-\left(k_1'+k_2'\right)(t-t_i)}\right] + \frac{k_2'}{k_1' + k_2' - k_3'} \left[e^{-k_3'(t-t_i)} - e^{-\left(k_1'+k_2'\right)(t-t_i)}\right] \right\} \tag{10}$$

And finally the cross-linking degree simply as:

$$\begin{aligned} \alpha = r_1 + r_2 = \beta & \left\{ \frac{k_1}{k_1 + k_2} \left[1 - e^{-(k_1+k_2)(t-t_i)}\right] + \frac{k_2}{k_1 + k_2 - k_3} \left[e^{-k_3(t-t_i)} - e^{-(k_1+k_2)(t-t_i)}\right] \right\} \\ & + (1-\beta) \left\{ \frac{k_1'}{k_1' + k_2'} \left[1 - e^{-\left(k_1'+k_2'\right)(t-t_i)}\right] + \frac{k_2'}{k_1' + k_2' - k_3'} \left[e^{-k_3'(t-t_i)} - e^{-\left(k_1'+k_2'\right)(t-t_i)}\right] \right\} \end{aligned} \tag{11}$$

Note that first derivative of (11) is:

$$\begin{aligned} \frac{d\alpha}{dt} = \beta & \left\{ k_1 e^{-(k_1+k_2)(t-t_i)} + \frac{k_2}{k_1 + k_2 - k_3} \left[-k_3 e^{-k_3(t-t_i)} + (k_1 + k_2)\, e^{-(k_1+k_2)(t-t_i)}\right] \right\} \\ & + (1-\beta) \left\{ k_1' e^{-(k_1+k_2)(t-t_i)} + \frac{k_2'}{k_1' + k_2' - k_3'} \left[-k_3' e^{-k_3'(t-t_i)} + \left(k_1' + k_2'\right) e^{-\left(k_1'+k_2'\right)(t-t_i)}\right] \right\} \end{aligned} \tag{12}$$

Normally constants $k_{1,2,3}$ and $k'_{1,2,3}$ are evaluated by least-squares best fitting [23]. A direct evaluation that needs very trivial numerical routines is proposed herein for the first time.

In Eq. (11), we make the hypothesis that:

$$\lim_{t \to +\infty} \alpha = \alpha_R = \beta \frac{k_1}{k_1 + k_2} + (1-\beta) \frac{k_1'}{k_1' + k_2'} \tag{13}$$

We also assume that at scorch the rate of vulcanization is α_0', i.e. from Eq. (12):

$$\left.\frac{d\alpha}{dt}\right|_{t=t_i} = \alpha_0' = \beta\,(k_1 + k_2) + (1-\beta)\left(k_1' + k_2'\right) \tag{14}$$

Note that (13) and (14) represent a system of two equations into two variables when $\beta = 1$ and $\beta = 0$. It is therefore necessary to perform two experimental tests at the same temperature with TBSS ($\beta = 1$) and DPG ($\beta = 0$) only, for the determination of k_1, k_2 and k_1', k_2'. In particular, when $\beta = 1$ we obtain:

$$\begin{cases} \alpha_R = \frac{k_1}{k_1+k_2} \\ \alpha_0' = k_1 + k_2 \end{cases} \Rightarrow \begin{cases} \alpha_R = \frac{k_1}{k_1+k_2} \\ \alpha_0' = k_1 + k_2 \end{cases} \Rightarrow \begin{cases} \alpha_0'\,\alpha_R = \alpha_0' - k_2 \\ k_1 = \alpha_0' - k_2 \end{cases} \Rightarrow \begin{cases} k_2 = \alpha_0'\,(1-\alpha_R) \\ k_1 = \alpha_0'\,\alpha_R \end{cases} \tag{15}$$

In case of $\beta = 1$ ($\beta = 0$), k_3 (k_3') constant is evaluated imposing the passage of curve (11) at t_P through α_P.

Mathematically such condition, for $\beta = 1$, reads as follows:

$$\alpha_P = \frac{k_1}{k_1+k_2}\left[1 - e^{-(k_1+k_2)(t_P - t_i)}\right] + \frac{k_2}{k_1+k_2-k_3}\left[e^{-k_3(t_P-t_i)} - e^{-(k_1+k_2)(t_P-t_i)}\right] \tag{16}$$

With the positions, $C_0 = \frac{k_1}{k_1+k_2}\left[1 - e^{-(k_1+k_2)(t_P-t_i)}\right]$, $C_1 = e^{-(k_1+k_2)(t_P-t_i)}$, $C_2 = k_2$, $C_3 = k_1 + k_2$ and $\bar{t}_P = t_P - t_i$, Eq. (16) may be re-written as follows:

$$\begin{aligned} \alpha_P &= C_0 + \frac{C_2}{C_3 - k_3}\left(e^{-k_3\bar{t}_P} - C_1\right) \\ &\Rightarrow \frac{(\alpha_P - C_0)\,(C_3 - k_3)}{C_2} = \left(e^{-k_3\bar{t}_P} - C_1\right) \end{aligned} \tag{17}$$

Assuming the following positions:

$$\begin{aligned} y_1 &= \frac{(\alpha_P - C_0)\,(C_3 - k_3)}{C_2} = -\frac{\alpha_P - C_0}{C_2}k_3 + \frac{\alpha_P - C_0}{C_2}C_3 \\ y_2 &= \left(e^{-k_3\bar{t}_P} - C_1\right) \end{aligned} \tag{18}$$

it has to be imposed that $y_1 = y_2$.

In the plane $k_3 - y_1$, y_1 is a straight line with negative slope and positive intersection with y_1-axis. Indeed, it can be easily proved that $\alpha_P - C_0 > 0$ since:

$$\alpha_P = C_0 + \frac{k_2}{k_1+k_2-k_3}\left[e^{-k_3(t_P-t_i)} - e^{-(k_1+k_2)(t_P-t_i)}\right] \tag{19}$$

and with the assumption that $k_3 < k_1 + k_2$, it turns out immediately that $e^{-k_3(t_P-t_i)} > e^{-(k_1+k_2)(t_P-t_i)}$

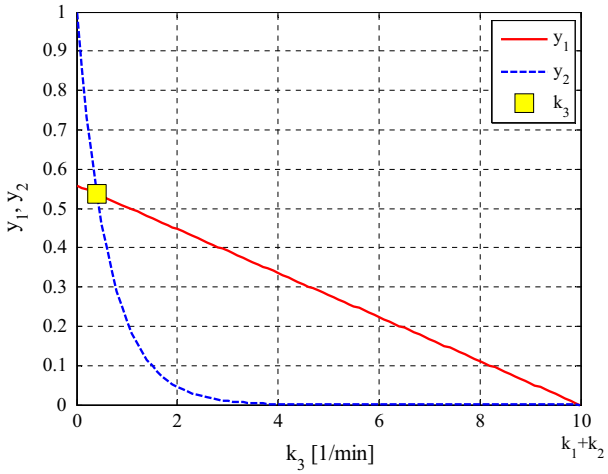

Fig. 5 Case with $y_1(0) < y_2(0)$

The second function y_2 is an exponential one, with the following properties:

$$\begin{aligned} & y_2(0) = 1 - e^{-(k_1+k_2)(t_P - t_i)} > 0 \\ & y_2(k_1 + k_2) = 0 \\ & \lim_{t \to +\infty} y_2 = -C_1 = -e^{-(k_1+k_2)(t_P - t_i)} \end{aligned} \tag{20}$$

Furthermore, it is interesting to notice that:

$$\begin{aligned} y_1(0) &= \frac{\alpha_P - C_0}{C_2} C_3 = \frac{\alpha_P - \frac{k_1}{k_1+k_2}\left[1 - e^{-(k_1+k_2)(t_P - t_i)}\right]}{k_2}(k_1 + k_2) \\ y_1(k_1 + k_2) &= \frac{\alpha_P - C_0}{C_2}(C_3 - k_1 - k_2) = 0 \end{aligned} \tag{21}$$

$y_1 = y_2$ always for $k_3 = k_1 + k_2$, which is not physically admissible, since reversion cannot be greater than the formation of the product undergoing reversion (k_2). However, an admissible solution is possible if $y_1(0) < y_2(0)$, as can be easily seen from Fig. 5.

After trivial algebra, it can be observed that:

$$\begin{aligned} y_1(0) &= \frac{\alpha_P - \frac{k_1}{k_1+k_2}\left[1 - e^{-(k_1+k_2)(t_P - t_i)}\right]}{k_2}(k_1 + k_2) \\ &= (k_1 + k_2)\frac{\alpha_P}{k_2} - \frac{k_1}{k_2} + \frac{k_1}{k_2} e^{-(k_1+k_2)(t_P - t_i)} \\ &= (k_1 + k_2)\frac{\alpha_P}{k_2} - \frac{k_1}{k_2} y_2(0) < y_2(0) \\ &\Leftrightarrow \alpha_P < y_2(0) = 1 - e^{-(k_1+k_2)\bar{t}_P} \end{aligned} \tag{22}$$

Inequality (22), taking into account equation (15) provides a condition for the point α_P to select:

$$\begin{aligned} \alpha_P &< 1 - e^{-\alpha_0' \bar{t}_P} \\ &\Rightarrow e^{-\alpha_0' \bar{t}_P} < 1 - \alpha_P \end{aligned} \tag{23}$$

When (as the cases here treated) it is not practically possible the evaluation of the single kinetic constants assuming a zero concentration of one of the accelerators, i.e. the experimental data for $\beta = 1$ and $\beta = 0$ are missing, it is worth noting that the model is capable of furnishing in closed form only a sort of "weighted sum" of each kinetic constant. In what follows, we will indicate with the symbols k_1, k_2 and k_3 such weighted sum coming from the numerical model, which does not refer directly to the case $\beta = 1$.

Also, it is important to underline that, when experimental data without one accelerator are at disposal (i.e. either $\beta = 1$ or $\beta = 0$ rheometer curves are available), the numerical determination of all the six constants is possible, firstly analyzing the rheometer curves without one accelerator and then any other case with a mixture of accelerators.

4 Numerical simulations

The reliability of the numerical procedure presented in the previous section, similarly to the validation done in [24], is tested on the normalized experimental rheometer data of Sect. 2, at two different concentrations of S–TBBS–DPG ingredients, respectively equal to 1-1-1 and 3-3-4 phr, as already discussed.

It is interesting to notice from experimental curves reported in Figs. 2 and 3, that in both cases the peak torque does not exhibit large variations at the different vulcanization temperatures tested. For this reason, it has been made the choice to normalize experimental data using Eq. (2), demonstrating in Fig. 4 that the obtained results are very similar to those provided by the rigorous procedure of Eq. (1).

The closed form solution provided by the authors for the kinetic scheme (3) in (15) excluding the induction period from the reactions (i.e. without an estimate of k_0 and k_0'), allows, after proper fitting of experimental data, the univocal determination of each kinetic constant at each temperature by means of closed form expressions, with the rather important advantage to allow circumventing the utilization of numerical demanding least squares optimization routines.

A comparison between normalized experimental curves and numerical predictions for NR+(S,TBBS,DPG)(3,3,4) system is depicted in Fig. 6 for vulcanization temperatures equal to 150 and 160 °C and in Fig. 7 for vulcanization temperatures equal to 170 and 180 °C.

A representation of functions y_1 and y_2 used to determine graphically kinetic constant k_3 is also provided for all vulcanization temperatures.

As can be noted, the experimental data fitting is almost perfect in the majority of the cases. The determination of the kinetic constants and the numerical curve are almost immediate, because only the solution of a two equations system (for k_1 and k_2) and of a non-linear single variable function (for k_3) is necessary.

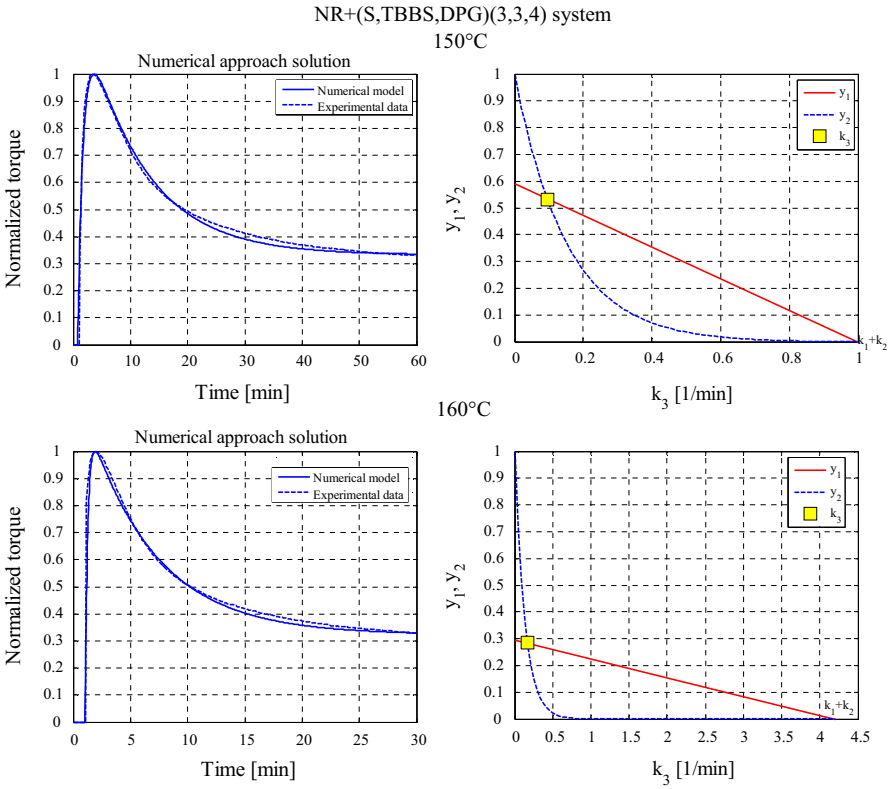

Fig. 6 NR+(S,TBBS,DPG)(3,3,4) system. Temperatures equal to 150 and 160 °C. *Left* Comparison between normalized cure-curves and numerical models. *Right* Graphical method to determine k_3 constant

The same comparisons are replicated respectively in Fig. 8 at temperatures equal to 150 and 160 °C and in Fig. 9 for curing temperatures equal to 170 and 180 °C for NR+(S,TBBS,DPG)(1,1,1) system.

Similarly to the previous case, the agreement between normalized experimental rheometer curves and predicted numerical ones is rather promising, with predictions of the kinetic constants obtained at a fraction of the time needed by any standard least squares approach available in the market.

Being experimental data at disposal for four increasing curing temperatures (namely 150, 160, 170 and 180 °C) for both the cases analyzed (S–TBBS–DPG equal to 3-3-4 and 1-1-1 phr, respectively), it is interesting to check if the kinetic constants found by means of the proposed numerical approach follow—at least in an approximate way—a linear behavior in the Arrhenius space, i.e. where the horizontal axis is represented by the inverse of the absolute curing temperature and the vertical axis is the logarithm of the kinetic constant.

Results for NR+(S,TBBS,DPG)(3,3,4) system are depicted respectively in Fig. 10 for k_1, in Fig. 11 for k_2 and Fig. 12 for k_3. The line represented in each figure is obtained by linear regression of the four numerical values of the constants coming

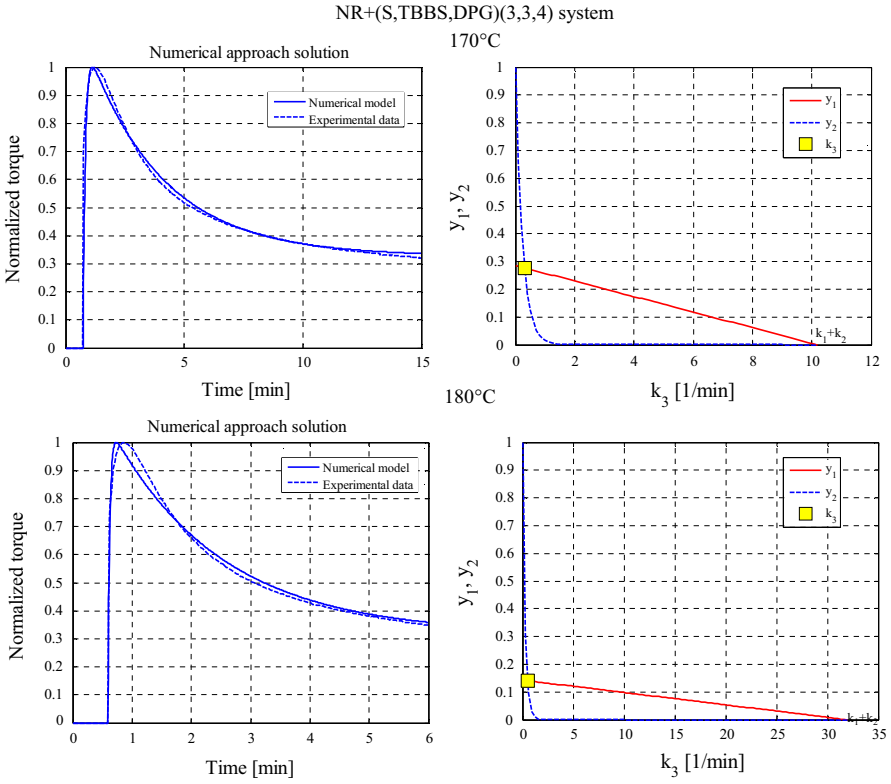

Fig. 7 NR+(S,TBBS,DPG)(3,3,4) system. Temperatures equal to 170 and 180 °C. *Left* Comparison between normalized cure-curves and numerical models. *Right* Graphical method to determine k_3 constant

from the proposed fitting, at different temperatures. It has the twofold advantage of: (1) providing the activation energy of the kinetic constant and, directly from the figure, (2) to show if the values found for k_i with the numerical procedure at the different temperatures follow the Arrhenius law, i.e. a first order temperature dependence of the reaction rates exists.

As can be systematically noted, for all constants, it appears that the trend is almost linear, confirming the robustness of the proposed model.

Similar considerations on kinetic constants hold also for the second case analyzed, i.e. for NR+(S,TBBS,DPG)(1,1,1) system. In particular, k_1 trend is depicted in Fig. 13, k_2 in Fig. 14 and k_3 in Fig. 15. Again, the linearity of the obtained results is worth noting and the same considerations done for the previous case studied hold.

From a detailed analysis of Fig. 16, where all the kinetic constants numerically found for the systems NR+(S,TBBS,DPG)(1,1,1) and NR+(S,TBBS,DPG)(3,3,4) are comparatively depicted, the following considerations may be done:

1. The activation energies for NR+(S,TBBS,DPG)(3,3,4) and NR+(S,TBBS,DPG)(1,1,1) are for k_1, k_2 and k_3, respectively equal to 45,330, 46,390, 24,943, 23,200, 19,200 and 25,600 cal/mol. Such numerical values indicate clearly that

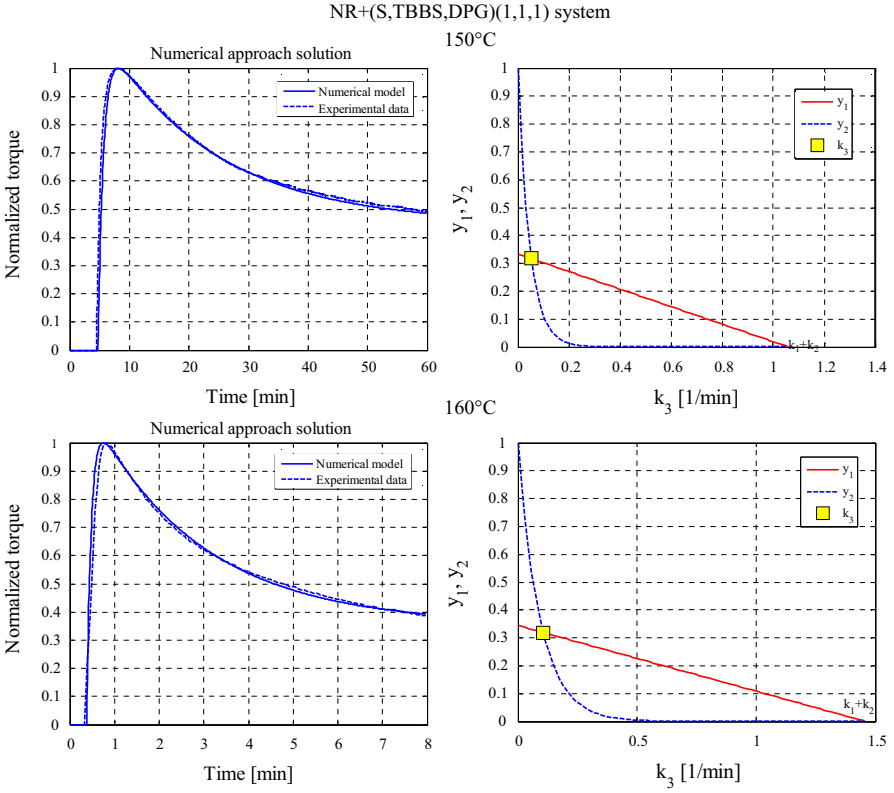

Fig. 8 NR+(S,TBBS,DPG)(1,1,1) system. Temperatures equal to 150 and 160 °C. *Left* Comparison between normalized cure-curves and numerical models. *Right* Graphical method to determine k_3 constant

reactions corresponding to higher activation energies exhibit faster rates at high temperatures.

2. In agreement with intuition, the numerical model confirms that k_2 values are systematically higher than k_1 ones, meaning that the reaction corresponding to the formation of the unmatured crosslinked polymer has a higher rate than that of the formation of the activated complex.
3. Considering the lowest vulcanization temperature (150 °C), k_1 and k_2 are very similar for both systems. However, k_1 and k_2 constants at the highest vulcanization temperature (180 °C) are 10 times greater for NR+(S,TBBS,DPG)(3,3,4) system.
4. k_1 and k_2 values found numerically for NR+(S,TBBS,DPG)(1,1,1) system are systematically lower and less sensitive to an increase of the vulcanization temperature than those found for NR+(S,TBBS,DPG)(3,3,4). Such numerical behavior is in agreement with the shape of the rheometer curves experimentally determined. In particular, it is interesting to notice that at the beginning of the vulcanization process, the first derivative of the experimental rheometer curves increases sensibly with the temperature for NR+(S,TBBS,DPG)(3,3,4), see Fig. 2, whereas it remain more constant for NR+(S,TBBS,DPG)(1,1,1), see Fig. 3. Such trend is probably a consequence of the lower crosslinking density.

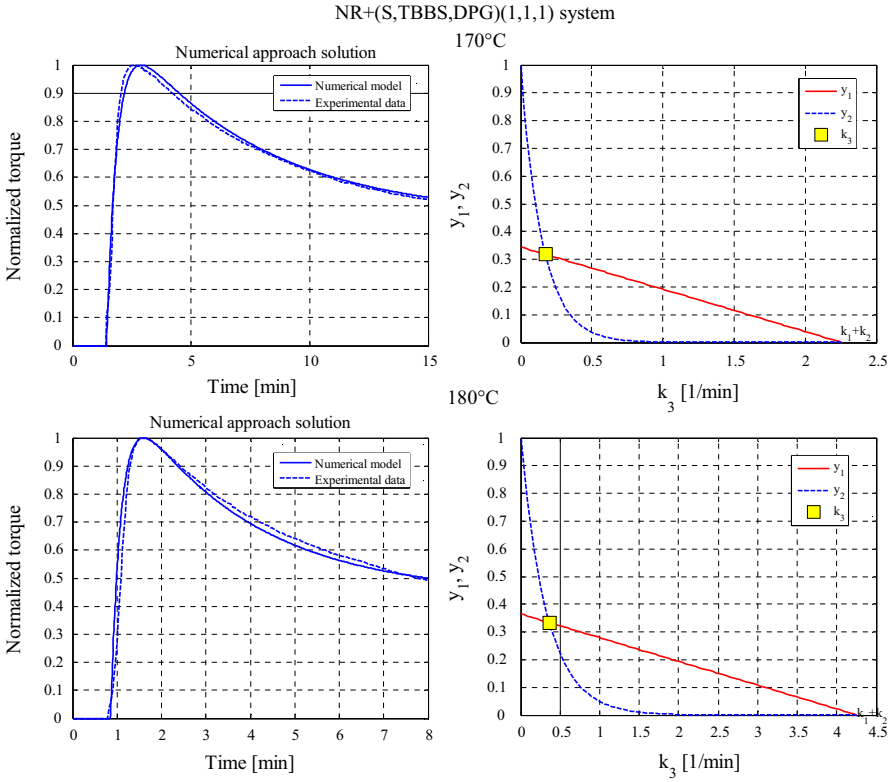

Fig. 9 NR+(S,TBBS,DPG)(1,1,1) system. Temperatures equal to 170 and 180 °C. *Left* Comparison between normalized cure-curves and numerical models. *Right* Graphical method to determine k_3 constant

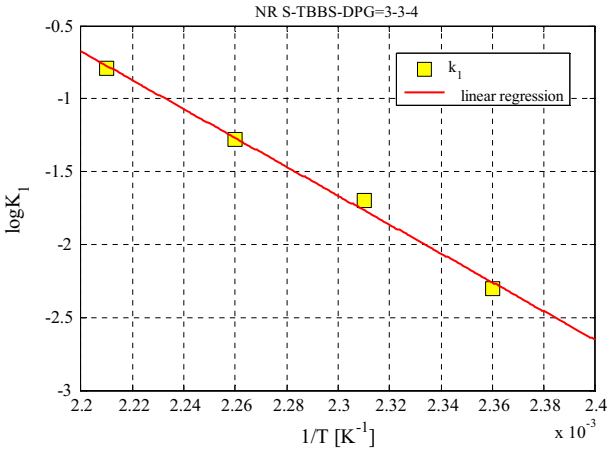

E_a=-2.3*1.99*slope=45330 cal/mol

Fig. 10 NR+(S,TBBS,DPG)(3,3,4) system, k_1 constant behavior at different temperatures in the Arrhenius space and estimated activation energy

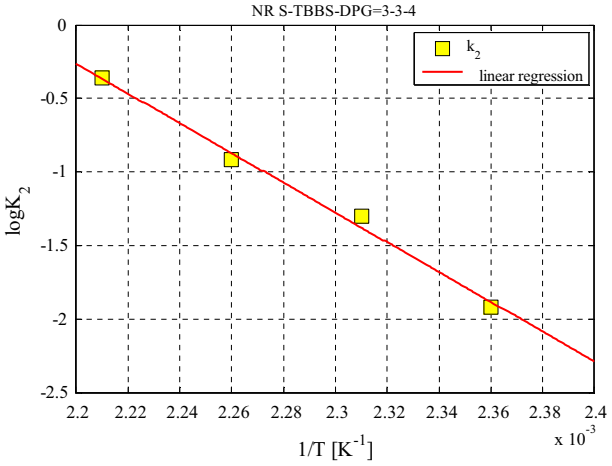

E_a=-2.3*1.99*slope=46390 cal/mol

Fig. 11 NR+(S,TBBS,DPG)(3,3,4) system, k_2 constant behavior at different temperatures in the Arrhenius space and estimated activation energy

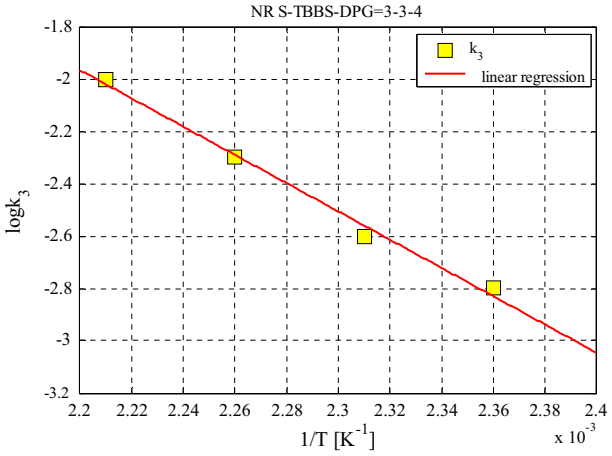

E_a=-2.3*1.99*slope=24943 cal/mol

Fig. 12 NR+(S,TBBS,DPG)(3,3,4) system, k_3 constant behavior at different temperatures in the Arrhenius space and estimated activation energy

5. The reversion reaction results quite slow, especially when compared with reactions related to k_1 and k_2 constants, and its variation with temperature seems not so much influenced by the variation of concentration among S–TBBS–DPG components. As expected, indeed, the activation energies for reversion for NR+(S,TBBS,DPG)(3,3,4) and NR+(S,TBBS,DPG)(1,1,1) systems have almost the same values, because the reversion percentage in both systems, see Tables 2 and 3, are similar and mainly due to the break of the multiple S–S bonds. To sys-

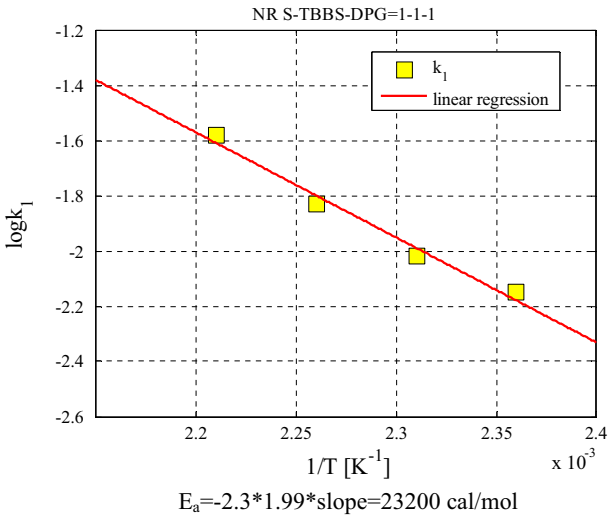

Fig. 13 NR+(S,TBBS,DPG)(1,1,1) system, k_1 constant behavior at different temperatures in the Arrhenius space and estimated activation energy

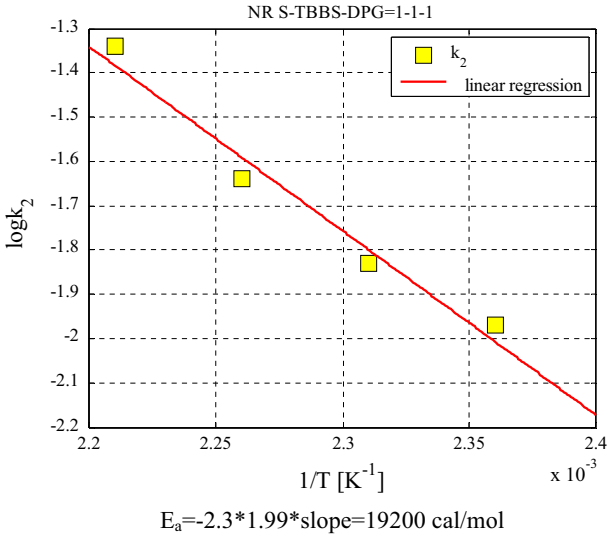

Fig. 14 NR+(S,TBBS,DPG)(1,1,1) system, k_2 constant behavior at different temperatures in the Arrhenius space and estimated activation energy

tematically confirm such conclusion, additional experimentation would however be required.

6. Numerical values of k_3 constants at a given vulcanization temperature for NR+(S,TBBS,DPG)(3,3,4) system are roughly twice the values found for NR+(S,TBBS,DPG)(1,1,1), being such property strictly connected to the absolute

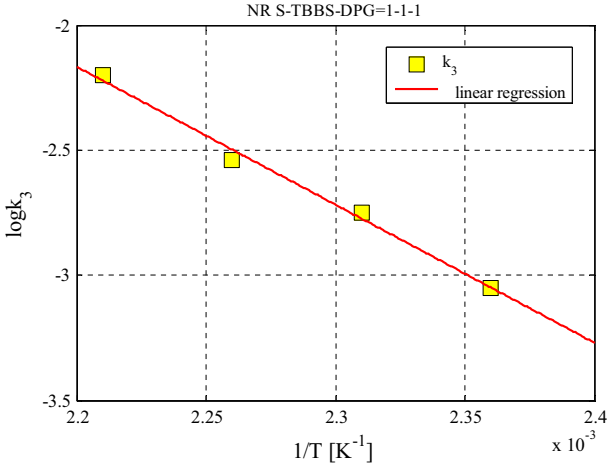

E_a=-2.3*1.99*slope=25600 cal/mol

Fig. 15 NR+(S,TBBS,DPG)(1,1,1) system, k_2 constant behavior at different temperatures in the Arrhenius space and estimated activation energy

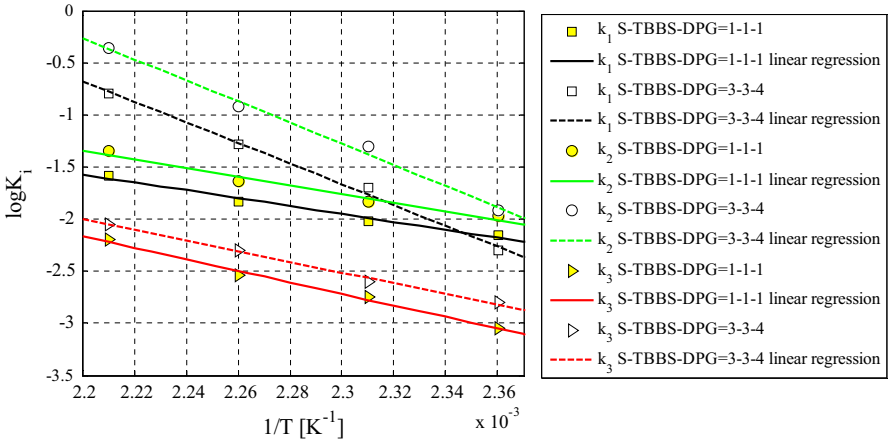

Fig. 16 Overall comparison among ki constants for the cases analyzed in the Arrhenius space

amount of S–S multiple bonds present. As already pointed out, the activation energies are however similar.

5 Conclusions

In this paper, we have studied from a numerical standpoint the crosslinking reactions occurring in NR added with only sulphur, TBBS and DPG accelerators in different concentrations. In this particular case, it has been made the simplified but technically meaningful assumption that there is no interaction between the additives used. This

assumption was derived in consideration of the quite similar molar ratio between the all activators and the sulphur.

Starting from previously presented models by the authors in this field, a detailed closed form approach with the straightforward analytical determination of kinetic constants of the model has been presented and discussed. The kinetic scheme is characterized by three main reactions per activator, occurring in series and parallel. The major improvement of the present approach when compared to existing literature is the derivation of a closed form expression for the crosslinking density and the determination of the kinetic constants without the need of utilizing least squares fitting routines. The model has been benchmarked on two series of experimental data at different concentrations of S, TBBS and DPG at four different temperatures. From simulations results, it was found that the kinetic constants follow reasonably well an Arrhenius law, which represents one of the most useful relationships in chemical kinetics, when an extrapolation of the behavior is needed outside the experimentally tested temperature range.

References

1. Y. Tanaka, Rubber Chem. Technol. **64**, 325 (1991)
2. G. Wolfman, Hasenhidl, S. Wolf, Kautsch. Gummi Kunstst. **44**(2), 118 (1991)
3. A.Y. Coran, *Science and Technology of Rubber, Chapter 7* (Academic Press, New York, 1978)
4. K.D.O. Jackson, M.J.R. Loadman, C.H. Jones, G. Ellis, Spectrochim. Acta **46**(2A), 217 (1990)
5. G. Ellis, P.J. Hendra, M.J.R. Loadman, Kautsch. Gummi Kunstst. **43**(2), 118 (1990)
6. D.J.P. Harrison, W.R. Yates, J. Macromol. Sci. C **25**, 481 (1985)
7. A.M. Zaper, J.L. Koenig, Rubber Chem. Technol. **60**, 252 (1987)
8. R. Orza, P.C.M.M. Magusin, V.M. Litvinov, M. van Duin, M.A.J. Michels, Macromolecules **42**, 8914–8924 (2009)
9. H.G. Dikland, M. van Duin, Crosslinking of EPDM and polydiene rubbers studied by optical spectroscopy, in *Spectroscopy of Rubbers and Rubbery Materials*, ed. by V.M. Litvinov, P.P. De (Rapra Technology Ltd., Shawbury, 2002). 207
10. T. Kemperman, Kautsch. Gummi Kunstst. **40**, 820 (1987)
11. E. Leroy, Souid, R. Deterre, Polym. Test. **32**, 575–582 (2013)
12. G. Milani, F. Milani, J. Appl. Polym. Sci. **119**, 419–437 (2011)
13. G. Milani, F. Milani, Polym. Test. **33**, 1–15 (2014)
14. R. Ding, I. Leonov, J. Appl. Polym. Sci. **61**, 455 (1996)
15. R. Ding, I. Leonov, A.Y. Coran, Rubber Chem. Technol. **69**, 81 (1996)
16. I.S. Han, C.B. Chung, S.J. Kang, S.J. Kim, H.C. Chung, Polymer (Korea) **22**, 223–230 (1998)
17. X. Colin, L. Audouin, J. Verdu, Polym. Degrad. Stab. **92**(5), 906–914 (2007)
18. M.R. Kamal, S. Sourour, Polym. Eng. Sci. **13**, 59–64 (1973)
19. G. Milani, E. Leroy, F. Milani, R. Deterre, Polym. Testing **32**, 1052–1063 (2013)
20. T. Hanel, Technical Report, *Vulcanization behavior of immiscible elastomer blends*. (Pirelli Tyre SpA, 2013)
21. X. Sun, A.I. Isayev, Rubber Chem. Technol. **82**(2), 149–169 (2009)
22. R.P. Quirk, Prog. Rubber Plast. Technol. **4**(1), 31 (1988)
23. Matlab User's Guide. http://www.mathworks.com/products/matlab/ (2007)
24. G. Milani, F. Milani, J. Math. Chem. **52**(2), 464–488 (2014)